Imprinting of nematic order at surfaces created by polymerization-induced phase separation

Karl R. Amundson
Bell Laboratories, Lucent Technologies, 600 Mountain Avenue, Murray Hill, New Jersey 07974
(Received 6 March 1998)

Surface interactions of liquid crystals at interfaces are crucial for the performance of devices that use liquid crystals. Many dispersions of polymers and liquid crystals for electro-optic applications are made by polymerization-induced phase separation into a nematic and a polymer gel component. Imprinting of nematic order onto polymer interfaces created in this way was studied. Imprinting renders the interface anisotropic so that the liquid crystal has a preferred in-plane orientation. The interface can be imprinted with nematic order when the polymer network is formed but not after. Also, imprinting survives an excursion through a temperature-driven anchoring transition. These observations argue that imprinting is due not to surface-adsorbed mesogens, but to an anisotropic arrangement of the polymer network at the interface. Surface imprinting affects electro-optic properties of polymer-dispersed liquid crystal films in this study and it can be manipulated by an external field during film formation. [S1063-651X(98)10809-7]

PACS number(s): 42.70.Df

I. INTRODUCTION

Surface interactions of liquid crystals at interfaces are scientifically interesting as well as crucial for electro-optic devices that use liquid crystals. In many cases the liquid crystal is in contact with a polymer either as an aligning layer as in twisted-nematic displays or as a structural component such as in dispersions of polymers and liquid crystals. One example is the polymer-dispersed liquid crystal (PDLC), which consists of micrometer scale liquid crystal drops (typically nematic) embedded within a polymer matrix. PDLC films are highly scattering because of the refractive index differences between drops and their surroundings and curvature of the nematic within drops. By aligning the liquid crystal in a sufficiently strong electric or magnetic field, the drops can appear index matched to their surroundings for light of normal incidence and the film becomes transparent [1–3]. Because of their switchable scattering power, they are used as switchable privacy windows for architectural applications and are candidate materials for flat panel displays. In another variation, the nematic drops are made to be much smaller than the wavelength of light to reduce scattering. The space-average refractive index can be modulated by field alignment of the nematic component and this action can be used to make electrically switchable photonic devices [4–6]. Several other dispersions created by polymerization-induced phase separation of polymers and liquid crystals have been developed with a variety of interesting electro-optical properties [3,7–9].

Electro-optical properties of PDLCs depend on bulk properties of the liquid crystal, geometric factors, and liquid crystal anchoring at the drop surfaces [3,10–12]. Surface anchoring arises because the interfacial energy of a nematic at a substrate is, in general, a function of the orientation of the nematic near the interface. The anisotropic component of the interfacial energy is called the surface anchoring energy $w(\mathbf{n};\nu,\xi)$, where $\mathbf{n}$ is the nematic director, ν is the surface normal, and ξ indicates a special in-plane surface direction. Whether a liquid crystal prefers to orient with the director $\mathbf{n}$ normal to the interface (*homeotropic* anchoring), in the plane of the interface (*homogeneous* anchoring), or along a tilted direction or directions depends upon subtle interactions that are not well understood. Unidirectional homogeneous alignment can be produced by rubbing a substrate [13–15] and homeotropic alignment by treating the bounding surfaces with amphiphilic alkyl compounds such as surfactants [16–20]. The less common tilted anchoring has been seen at a glass surface exposed to smoke soot [21] or coated with a commercial fluorinated surfactant (Fluorad 431) [22].

At an isotropic surface, anchoring energy can depend only upon the angle between the nematic director and the surface normal. Interestingly, several studies have shown that certain initially isotropic surfaces can be rendered anisotropic by contact with an anisotropic phase. This phenomenon has been coined *surface memory* by Clark [23]. Friedel [24] in 1922, showed that crystals on clean glass imprinted their orientation on the surface and the nematic phase resulting from melting of the crystals aligned in directions defined by the crystals. Clark investigated a similar phenomenon at various polymer surfaces [23]. He reported a surface memory when smectic phases were formed in contact with hydrophobic polymers. No memory was observed for nematics or hydrophilic polymers. More recently, surface memory at a poly(vinyl alcohol) surface has been reported [25].

Ouchi *et al.* [26] used second harmonic generation and ellipsometry to study the orientation of octylcyanobiphenyl at a polyimide surface. They inferred that surface memory in that system was caused by mesogens adsorbed on the surface and trapped in local rotational potentials. Notably, they found only a very slightly anisotropic orientation of mesogens at a surface that exhibited memory.

Whether surface memory is present in some PDLC films has been an issue of speculation. Margerum *et al.* [27] reported on a memory phenomenon in PDLC films made by photopolymerization-induced phase separation of a mixture of the commercial liquid crystal E7 (EM Industries) and an ultraviolet-light-curable monomer mixture. In each experiment, two matching films were photopolymerized with one in an aligning electric or magnetic field (referred to as the field-cured film). The field-cured film exhibited several dif-

ferences from its counterpart. The voltage required to switch the field-cured film was lower and at zero field it was less scattering, giving a greater forward transmittance. These effects could have morphological origins: Perhaps the electric and magnetic fields elongate drops or could arise from imprinting of the nematic direction at the drop surface when the drops were formed. The latter explanation was preferred because the enhancement of forward transmittance through the field-cured film diminished upon heating the films within a couple of degrees of the nematic-to-isotropic temperature (T_{NI}). However, the E7 liquid crystal was later reported to have a biphasic (nematic plus isotropic) temperature range of 1.5 K (and presumably greater in the presence of impurities) just below T_{NI}. In this range, the drops become biphasic, with a nematic component enveloped in an isotropic fluid shell [11]. This would certainly eliminate the effects of surface memory at the polymer surfaces, but would also eliminate morphological effects, as surface tension drives the nematic component of a biphasic drop to a spherical shape.

Yamaguchi and Sato [28,29] observed persistent states in bicontinuous polymer/liquid crystal dispersions, but the persistence was small or absent in related PDLC films. One notable characteristic is that the memory in these structures is erasable by heating the film into the isotropic state. It seems likely that persistence in these cases arises from multiple metastable nematic director patterns associated with the bicontinuous morphologies.

In this paper imprinting of nematic order at surfaces created by polymerization-induced phase separation is demonstrated. The vehicle for this study is electric field alignment of nematic order during formation of PDLC films. Pairs of identical PDLC films were formed where an electric field aligned the nematic director in one film while in the other the director orients in various directions according to drop shapes. Differences in electrical and optical properties of the two films reveal a memory of the early director orientation in some cases. The dependence of memory on surface anchoring shows that memory in the film is associated with the drop surfaces. Characteristics about surface anchoring are gained from studying the effect of surface anchoring on memory, from thermal studies, and from passage through a temperature-induced anchoring transition.

II. EXPERIMENT

PDLC films were made from a mixture of ~80 wt. % liquid crystal (TL205, EM Industries) and ~20 wt. % UV-curable acrylate monomer. TL205 is a mixture of halogenated bi- and terphenyls with aliphatic tails of lengths two to five carbon atoms [18]. The monomer mixture is mostly (85 wt. %) monofunctional alkyl acrylate with a polyfunctional acrylate (13.5 wt. %, 1,1,1-trimethylol propane triacrylate) to add cross links to the polymer network and a UV sensitive photoinitiator (1.5 wt. %, Darocur 1173, Ciba). The choice of monofunctional acrylate was varied to achieve the desired anchoring transition temperature. The mixture was placed between two indium-tin-oxide-coated glass plates separated by 10–20 μm and then cured with UV light. Upon polymerization, the solution supersaturates. Drops of nematic liquid crystal form and are held in place by solidification of the matrix.

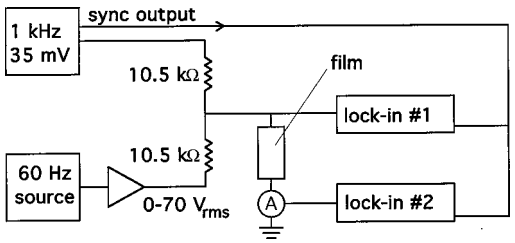

FIG. 1. Electrical impedance measurement apparatus. Lock-in 1 measures the voltage at 1 kHz and lock-in 2 measures the current amplitude and phase at 1 kHz.

To study the effect of an electric field during curing, pairs of otherwise identical films were prepared simultaneously. Across one, a sinusoidal (1 kHz) voltage was applied throughout photopolymerization and it is referred to as the field-cured film. The other is called the reference film.

The forward transmittance of a HeNe laser beam (632.8 nm) passing normally through the film was measured using 2° (full angle) collection optics. The film temperature was controlled with a Mettler FP82 hot stage with cold nitrogen gas flow. Electrical impedance across the film was determined by measuring the amplitude and phase of current passing through the film at 1 kHz while applying a 1-kHz voltage signal (Fig. 1). The test voltage was kept small ($\sim 18\ \mathrm{mV_{rms}}$) so as to not perturb the nematic director. The impedance was also measured when the nematic was well aligned by a large-amplitude 60-Hz voltage. In that case, the 60-Hz aligning voltage was mixed with a 1-kHz test voltage and the current at 1 kHz only was measured.

III. RESULTS AND DISCUSSION

A. Control of surface anchoring

The formulation used to make PDLC films studied here was recently discovered in this laboratory [12] to exhibit anchoring behavior that depends sensitively on the nature of the polymer side group. In general, anchoring was found to be homeotropic at low temperature and homogeneous at high temperature (see Fig. 2), with an anchoring transition temperature T_t that depends on the structure of the polymer side group, as shown in Table I of Ref. [12]. In general, long, linear alkyl side groups induce homeotropic anchoring up to close to the nematic-to-isotropic transition temperature of about 84 °C in the PDLC films. Decreasing the length of the side group causes T_t to decrease somewhat, but use of a branched, secondary or cyclic alkyl side group induces a much more dramatic drop in T_t. Intermediate values of T_t can be obtained by mixing one or more monofunctional acrylates in the PDLC formulation, resulting in copolymers with a mix of side groups.

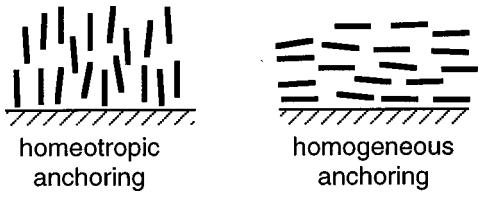

FIG. 2. Homeotropic and homogenous anchoring of a nematic liquid crystal at an interface.

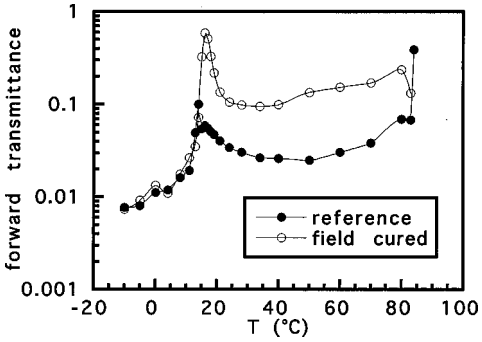

FIG. 3. Forward transmittance through the field-cured and reference films made using a 75-25 wt. % mix of isobornyl acrylate and *n*-octyl acrylate. Transmittance is relative to transmission through the optical apparatus without a sample.

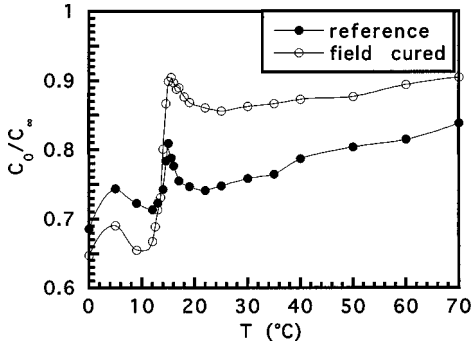

FIG. 4. C_0/C_∞ for the field-cured and reference films made with a 75-25 wt. % mix of isobornyl acrylate and *n*-octyl acrylate.

This formulation offers a crucial feature for this work, namely the ability to affect anchoring without large changes in morphology. The morphology varies only slightly with the choice of alkyl acrylate because the solubility of the liquid crystal in all acrylate matrices used here is similar.

B. Memory of field alignment and the anchoring condition

Two PDLC films with thicknesses of $20\pm1\ \mu$m were made using a 75-wt. % isobornyl acrylate and 25-wt. % *n*-octyl acrylate mixture as the monofunctional acrylate component. This mixture of monofunctional acrylates yields PDLC films with an anchoring transition temperature at 14 °C, and anchoring is homeotropic below 14 °C and homogeneous above. PDLC films were made at ambient temperature, 23 ± 1 °C and anchoring is homogeneous at that temperature. A 53 V_{rms} 1-kHz voltage was applied across one film during photopolymerization.

One concern is that drops could be elongated by the action of an electric field. This has been observed in phase separated polymer blends [30]. Impedance measurements show that at the 1-kHz frequency used the films are purely dielectric. Therefore, the theoretical analysis of static drop shape in an electric field by Garton and Krasucki is relevant [31]. Assuming a surface energy on the order of 10 ergs/cm^2, their theory predicts that the electric field used would not significantly elongate the drops. To explore this possibility, a second pair of films was made from the same mixture with a trace amount of fluorescent dye (Pyrromethene 580; Exciton Chemical Co., Dayton, Ohio) and was studied by fluorescence confocal microscopy. The morphology of the field-cured and reference film had a similar appearance.

After photopolymerization, the voltage was removed and the zero-voltage forward transmittance through the two films was measured as a function of temperature (Fig. 3). Across the entire temperature range where anchoring is homogeneous, the forward transmittance through the field-cured film exceeds its counterpart by a factor of 3–5. Upon cooling the films below 14 °C, the surface anchoring changes to homeotropic and the forward transmittance through the pair of films becomes similar.

The enhanced forward transmittance in the field-cured film above 14 °C suggests that the nematic director distribution is biased toward greater alignment with the film normal than in the reference film, that is, the film is ''partially switched'' even in zero field. Impedance measurements confirm this. Measurements were made on a second pair of films made with the same formulation and procedure but with a smaller surface area (presumably because of the finite resistance of the indium-tin-oxide surface electrodes, the smaller films gave better impedance results). The impedance is reactive (phase angle 88°–90°) so to a good approximation it can be considered purely capacitive. The capacitance of the film can be expressed as

$$C=\frac{\varepsilon_{\mathrm{eff}}A}{d}, \tag{1}$$

where A is the surface area of the overlapping parts of the electrodes, d the gap thickness, and $\varepsilon_{\mathrm{eff}}$ the effective dielectric constant. The capacitance both at zero excitation voltage (C_0) and at an excitation voltage that saturates both the capacitance and forward transmittance (C_∞) was measured. C_∞ varied only very slowly with temperature. Geometric contributions to the capacitance are canceled by taking the ratio C_0/C_∞, which is plotted as a function of temperature in Fig. 4. When, in zero field, the nematic liquid crystal is not well aligned with the film normal, C_0 is small as is the ratio C_0/C_∞. This ratio increases toward unity as the zero-field director is more strongly aligned with the film normal. Above the anchoring transition temperature, the field-cured film has a significantly larger capacitance ratio, indicating better alignment in zero field. Below 14 °C where the anchoring is homeotropic, C_0/C_∞ for the field-cured film is about 10% lower than the reference film, suggesting more in-plane alignment of the director in the field-cured film. This surprising observation is repeatable, but the reason for it is unknown.

The forward transmittance and the capacitance ratio exhibit peaks at the anchoring transition temperature. Both can be attributed to a relaxation of the internal drop structure near the transition. Light is scattered by spatial variations in the refractive index tensor, especially variations with length scale near the wavelength of light. One contribution is curvature of the director field within the drops. Near the anchoring transition, anchoring becomes weak and so the director field in the drops becomes less curved [9]. This loss of internal structure means that less light is scattered and more light is transmitted in the forward direction.

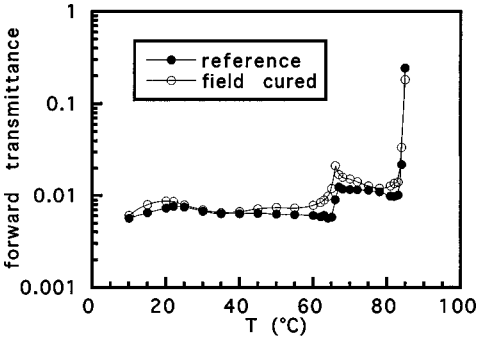

FIG. 5. Forward transmittance through the field-cured and reference films made using *n*-hexyl acrylate.

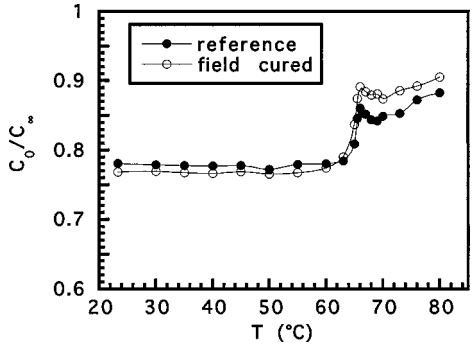

FIG. 6. C_0/C_∞ for the field-cured and reference films made with *n*-hexyl acrylate.

The peak in the ratio C_0/C_∞ arises for a similar reason, namely, near the anchoring transition the director field in the drops loses internal structure. A calculation of ε_{eff} for a PDLC film is given in the Appendix. To second order in the spatial variations of the dielectric tensor $\delta\underset{\approx}{\varepsilon}=\underset{\approx}{\varepsilon}(\mathbf{r})-\langle\underset{\approx}{\varepsilon}(\mathbf{r})\rangle$, the effective capacitance is given by

$$\varepsilon_{\text{eff}}=\hat{\mathbf{e}}_z\cdot\langle\underset{\approx}{\varepsilon}(\mathbf{r})\rangle\cdot\hat{\mathbf{e}}_z-\int\frac{[\hat{\mathbf{e}}_k\cdot\tilde{\delta}\underset{\approx}{\varepsilon}(\mathbf{k})\cdot\hat{\mathbf{e}}_z]^2}{\hat{\mathbf{e}}_k\cdot\langle\underset{\approx}{\varepsilon}(\mathbf{r})\rangle\cdot\hat{\mathbf{e}}_k}\,d^3\mathbf{k}, \qquad (2)$$

where the overhead tilde denotes a Fourier transform with wave vector $\mathbf{k}$ and the angular brackets denote a spatial average over the film. The first term gives the space average of the dielectric tensor projected onto the film normal $\hat{\mathbf{e}}_z$. The second term is an integration over normalized Fourier components of the dielectric tensor and acts to diminish ε_{eff}. In weak anchoring, the curvature of the director field is reduced and so contributions to the second term are also reduced, giving an increase in the effective capacitance. For this reason, there will be a peak in C_0/C_∞ around the anchoring transition temperature with a width that corresponds to the temperature range of weak anchoring. Given the liquid crystal dielectric anisotropy ($\varepsilon_{\text{par}}=9.1$ and $\varepsilon_{\text{perp}}=4.1$ at 24 °C), the magnitude of the peak in C_0/C_∞, far from T_{NI}, should be on the order of 10% of its base line value. Since the dielectric anisotropy diminishes as T_{NI} is approached, films with an anchoring transition temperature closer to T_{NI} should exhibit a smaller peak in C_0/C_∞, as is seen in the next example.

The same experiment was repeated on another set of PDLC films for which *n*-hexyl acrylate was used as the monofunctional acrylate component. The rate of structure formation and the final structure is similar to that of the films made with the mixture of isobornyl and *n*-octyl acrylates. The films made with *n*-hexyl acrylate exhibit an anchoring transition at 65 °C so anchoring is homeotropic during photopolymerization, which takes place at room temperature. The forward transmittance through the two films are shown in Fig. 5. There is only a slight enhancement in forward transmittance for the field-cured film near the anchoring transition temperature, but the difference is dwarfed by the large difference shown by the previous set of films. The ratio C_0/C_∞, shown in Fig. 6, is also very similar for the two films. Below the anchoring transition temperature, C_0/C_∞ is about 1% smaller and above it is about 3% greater.

The data show that the field-induced memory is strong when anchoring is homogeneous during film formation and nearly absent when anchoring is homeotropic during film formation. This argues against a morphological basis to the memory (e.g., field-induced elongation of drops) because bulk forces are insensitive to surface anchoring. Consider a single nematic drop in an aligning field (Fig. 7). The nematic is well aligned through the bulk of the drop and only over a thin boundary layer near the surface does the director bend to accommodate the surface anchoring condition. When the boundary layer is much smaller than the drop radius, its thickness can be estimated from the calculated boundary layer thickness at a flat surface [32]

$$\xi\sim\left(\frac{4\pi K}{\Delta\varepsilon E^2}\right)^{1/2}, \qquad (3)$$

where K is the nematoelastic constant and $\Delta\varepsilon$ the dielectric anisotropy. For approximate field strengths and nematic properties, ξ is on the order of 100 nm at room temperature and smaller above room temperature.

Because the ability to impose a field-induced memory is sensitive to anchoring and because surface alignment is screened from the liquid crystal in the drop except for the boundary layer very close to the surface, the memory must reside within the surface-aligned boundary layer and presumably at the drop surface. In addition, the ability to imprint a special direction onto a surface requires a break in azimuthal symmetry. A homogeneously anchored nematic defines a

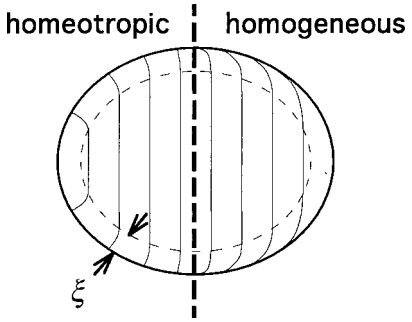

FIG. 7. A single drop of nematic is represented. The lines denote the nematic director in a strong aligning electric field. In the left half anchoring is homeotropic and on the right it is homogeneous. The director field bends to accommodate surface anchoring in a boundary layer of thickness ξ near the drop surface.

special direction at the surface and imprinting is possible. In strong homeotropic anchoring azimuthal surface symmetry is maintained and a special direction cannot be defined. However, if the homeotropic anchoring is sufficiently weak that the electric field induces a small tilt of the director at the surface, then azimuthal symmetry can be broken and imprinting of a special direction is again possible. The magnitude of the tilt can be estimated by balancing the electric field torque throughout the boundary layer of misalignment near a flat surface:

$$\sin\,\theta_{\text{tilt}} \sim \frac{K}{w_0 \xi} \equiv \left(\frac{\Delta\varepsilon E^2 K}{4\pi}\right)^{1/2} \frac{1}{w_0}, \tag{4}$$

where w_0 is the surface anchoring energy and θ_{tilt} is the tilt angle. Memory of a special direction should be slight for small tilt angles. It is notable that signatures of surface imprinting are not completely absent from the film made with *n*-hexyl acrylate. Perhaps a surface imprinting is permitted by a field-induced tilt away from homeotropic anchoring. Another explanation, however, is that anchoring is not exactly homeotropic, but slightly tilted from normal. Discerning a small tilt angle would be difficult.

C. Surface imprinting and thermal cycling

Clues about the molecular basis for surface imprinting can be gained from several thermal cycling experiments. It is helpful at this point to consider a couple of molecular models. Ouchi *et al.* [26] proposed that, for octylcyanobiphenyl on a polyimide surface, mesogens adsorb on the surface and are trapped in rotational potential wells caused by local polymer conformations. Memory is then maintained in an anisotropic distribution of the adsorbed surface layer of mesogens and the polymer is uninfluenced by the nematic phase. For the materials in this study, the polymer is formed while in contact with a nematic phase. It is therefore possible that the nematic director is imprinted upon the polymer gel network and that imprinting is made permanent by cross linking. Memory is then maintained by an anisotropic distribution of polymer chains segments and/or spatial correlation of functional groups in the network at the drop interface. This mechanism has similarities to the principles behind cross-linked molecular templates [33].

Access to an anchoring transition allows a simple test to distinguish between these two models. Mesogens lying with their long axes in the plane of the surface in homogeneous anchoring are caused to stand up at the interface upon cooling to homeotropic anchoring. Then mesogens adsorbed on the polymer interface would certainly escape the rotational potentials they experience when lying flat on the interface. On the other hand, if the memory is retained in the polymer network at the interface, then the memory would survive the excursion to homeotropic anchoring. Electro-optic differences between the field-cured and reference films persist after cooling the films well into the homeotropic anchoring regime and then heating back up to the homogeneous anchoring regime. This shows that the memory survives the anchoring transition, supporting the model where memory is retained in the polymer network.

If memory is imprinted in a polymer network during cross linking, then imprinting would be impossible after the polymer network is formed. To test this, an attempt was made to write a field-aligned nematic order into a film *after* photopolymerization. The reference film used in the above experiment (made with *n*-hexyl acrylate monomer) was heated to 90 °C and then cooled at −1 °C/min to room temperature in an aligning electric field. The film shows no significant change in the forward transmittance or C_0/C_∞ across the entire temperature range (Fig. 8). The film is susceptible to imprinting during polymerization, but not after the polymer network is formed. Presumably, after the polymer chain segments are cross linked into a network, their orientation statistics cannot be rearranged by the nematic liquid crystal.

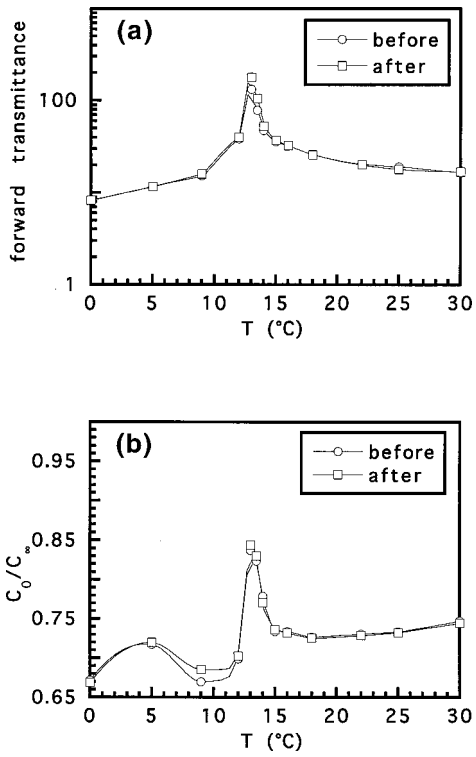

FIG. 8. (a) Forward transmittance and (b) C_0/C_∞ before and after slow cooling in an aligning electric field.

Films were heated to elevated temperatures both above and below the nematic-to-isotropic transition temperature to characterize the thermal stability of surface imprinting. Results are shown in Fig. 9. The two PDLC films in this experiment were made using the 75-25 isobornyl acrylate/*n*-octyl acrylate mixture of monofunctional acrylates described earlier so that T_t is at 14 °C. One film was cured in an aligning field and the other without a field. The forward transmittance and C_0/C_∞ were recorded after photopolymerization, then after heating for 1 h at 70 °C (below T_{NI}), and then again after heating for 1 h at 90 °C (above T_{NI}). The field-cured film was also held for an additional 4 h at 90 °C. Since the two films did not have exactly the same thickness, differences in absolute values of forward transmittance should be discounted. For the reference film, the peaks in both the forward transmittance and capacitance ratio C_0/C_∞ associated with the anchoring transition at T_t change, but values far from T_t change very little. Similar changes in the peak at T_t are also seen in the field-cured film, but in addition there is a significant downward drift in the data above T_t where anchoring is homogeneous. The decrease in C_0/C_∞ above T_t

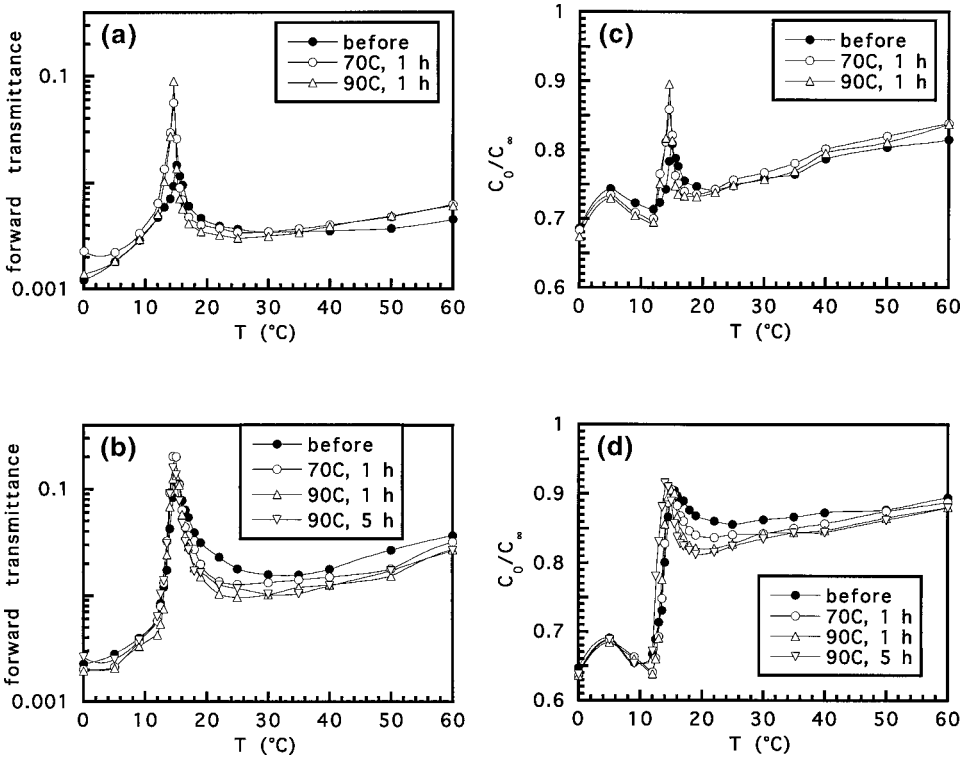

FIG. 9. Forward transmittance through (a) reference and (b) field-cured film before thermal treatment and then after holding at 70 °C for 1 h, followed by 90 °C for 1 h. The field-cured film was also held at 90 °C for an additional 4 h. (c) and (d) show C_0/C_∞ for the same thermal treatment.

for the field-cured film after thermal excursions indicates a lessening of the effect of surface imprinting. At least over the duration of these thermal excursions, surface imprinting is somewhat reduced, but not eliminated. In previous reports on surface memory, memory was shown to decay upon heating above the nematic-to-isotropic transition temperature [23,25,26]. In this work, surface imprinting effects diminish only a little as a result of holding the material above T_{NI}. This likely reflects the different physical bases for surface imprinting between the previous work, where the polymer surfaces were created before being put in contact with the nematic, and this study, where the polymer surface forms and the polymer is cross-linked while in contact with a nematic.

IV. CONCLUSIONS

Surface imprinting of liquid crystal orientation at surfaces created by polymerization-induced phase separation has been studied. The vehicle for this study is field alignment during formation of polymer-dispersed liquid crystal films. That memory of field alignment occurs at the drop interfaces was demonstrated by showing that memory is strong only when surface anchoring is homogeneous. When anchoring is homeotropic during film formation, signatures of the field-alignment memory are very slight. That surface imprinting survives a transition from homogeneous to homeotropic and back to homogeneous surface anchoring is evidence that the surface memory is held in the polymer network at the drop surface instead of in surface-adsorbed mesogens. Further evidence comes from the fact that surface imprinting does not occur after the polymer network is formed. Also, the signatures of surface memory diminish only slightly after holding the films at elevated temperatures. Surface imprinting is an important contributor to electro-optic properties of PDLC films and it can be manipulated by an external field during film formation.

ACKNOWLEDGMENT

The author thanks Mohan Srinivasarao for helpful discussion.

APPENDIX: CAPACITANCE AND PDLC FILM STRUCTURE

The capacitance of the PDLC film is given by Eq. (1). ε_{eff} is the dielectric constant of a hypothetical uniform and isotropic material that maintains the film capacitance when it replaces the PDLC material in the capacitor. It is given by equating the electrostatic energy across this hypothetical replacement

$$\frac{1}{8\pi}\,\varepsilon_{\text{eff}}|\mathbf{E}_0|^2=\frac{1}{8\pi}\,\frac{1}{\mathcal{V}}\int_{\mathcal{V}}\mathbf{E}(\mathbf{r})\cdot\underset{\approx}{\varepsilon}(\mathbf{r})\cdot\mathbf{E}(\mathbf{r})d^3\mathbf{r}, \quad \text{(A1)}$$

where $\mathbf{E}_0$ is given by

$$\mathbf{E}_0=\frac{V}{L}\,\hat{\mathbf{e}}_z, \quad \text{(A2)}$$

where V is the voltage across the film, L the gap thickness, and $\hat{\mathbf{e}}_z$ the unit vector normal to the substrates. $\mathcal{V}$ is the volume of integration and $\underset{\approx}{\varepsilon}(\mathbf{r})$ and $\mathbf{E}(\mathbf{r})$ are the spatially vary-

ing dielectric tensor and electric field, respectively. The dielectric tensor is spatially varying because of variations in both composition and orientation of the nematic director. For simplicity, Eq. (A1) is solved by perturbation analysis even though the variations in the dielectric constant can be as much as 50% the mean dielectric constant. The dielectric tensor can be separated into a space average $\langle \underset{\approx}{\varepsilon} \rangle$ and a spatially varying component $\delta \underset{\approx}{\varepsilon}$:

$$\underset{\approx}{\varepsilon}(\mathbf{r}) \equiv \langle \underset{\approx}{\varepsilon} \rangle + \delta \underset{\approx}{\varepsilon}(\mathbf{r}). \tag{A3}$$

By Fourier transform of Maxwell's electrostatic equations $\nabla \times \mathbf{E}(\mathbf{r}) = 0$ and $\nabla \cdot [\varepsilon(\mathbf{r})\mathbf{E}(\mathbf{r})] = 0$ and Eq. (A3), the Fourier transform of the electric field $\tilde{\mathbf{E}}(\mathbf{k})$ can readily be obtained. To first order in $\delta \underset{\approx}{\varepsilon}$, $\tilde{\mathbf{E}}(\mathbf{k})$ is given by

$$\tilde{\mathbf{E}}(\mathbf{k}) = \mathbf{E}_0 - \frac{\hat{\mathbf{e}}_k \cdot \tilde{\delta} \underset{\approx}{\varepsilon}(\mathbf{k}) \cdot \mathbf{E}_0}{\hat{\mathbf{e}}_k \cdot \langle \underset{\approx}{\varepsilon} \rangle \cdot \hat{\mathbf{e}}_k} \hat{\mathbf{e}}_k, \tag{A4}$$

where $\tilde{\delta} \underset{\approx}{\varepsilon}(\mathbf{k})$ is the Fourier transform of $\delta \underset{\approx}{\varepsilon}$ and $\hat{\mathbf{e}}_k$ is the unit wave vector. Only first-order contributions to the electric field contribute to the effective dielectric constant to second order in $\delta \underset{\approx}{\varepsilon}$. Equations (A3) and (A4) inserted into Eq. (A1) give the effective dielectric constant to second order in $\delta \underset{\approx}{\varepsilon}$:

$$\varepsilon_{\text{eff}} = \hat{\mathbf{e}}_z \cdot \langle \underset{\approx}{\varepsilon} \rangle \cdot \hat{\mathbf{e}}_z - \frac{1}{\mathcal{V}} \int \frac{(\hat{\mathbf{e}}_k \cdot \tilde{\delta} \underset{\approx}{\varepsilon} \cdot \hat{\mathbf{e}}_z)^2}{\hat{\mathbf{e}}_k \cdot \langle \underset{\approx}{\varepsilon} \rangle \cdot \hat{\mathbf{e}}_k} d^3\mathbf{k}. \tag{A5}$$

The effective dielectric constant to lowest order is given by the spatial average dielectric tensor projected onto the film normal, minus a term arising from the spatial variations in the dielectric constant. It is primarily the first term that rises as the liquid crystal is oriented with the electric field. The second term represents a negative contribution from compositional variations (contrast between drop and matrix) and from spatial variations in the nematic director.

[1] P. S. Drzaic and A. Muller, Liq. Cryst. **5**, 1467 (1989).
[2] J. W. Doane, MRS Bull. **16**, 22 (1991).
[3] P. S. Drzaic, *Liquid Crystal Dispersions* (World Scientific, Singapore, 1995).
[4] R. L. Sutherland, L. V. Natarajan, V. P. Tondiglia, and T. J. Bunning, Chem. Mater. **5**, 1533 (1993).
[5] R. L. Sutherland, V. P. Tondiglia, L. V. Natarajan, T. J. Bunning, and W. W. Adams, Appl. Phys. Lett. **64**, 1074 (1994).
[6] V. P. Tondiglia, L. V. Natarajan, R. L. Sutherland, T. J. Bunning, and W. W. Adams, Opt. Lett. **20**, 1325 (1995).
[7] D. K. Yang, L.-C. Chien, and J. W. Doane, Appl. Phys. Lett. **60**, 3102 (1992).
[8] D. K. Yang, J. L. West, L.-C. Chien, and J. W. Doane, J. Appl. Phys. **76**, 1331 (1994).
[9] C. N. Bowman and C. A. Guymon, MRS Bull. **22**, 15 (1997).
[10] J. H. Erdmann, S. Zumer, and J. W. Doane, Phys. Rev. Lett. **64**, 1907 (1990).
[11] K. Amundson, Phys. Rev. E **53**, 2412 (1996).
[12] K. Amundson and M. Srinivasarao, Phys. Rev. E **58**, R1211 (1998).
[13] H. E. W. Zocher and K. Coper, Z. Phys. Chem., Stoechiom. Verwandtschaftsl. **132**, 295 (1928).
[14] P. Chatelain, Bull. Soc. Fr. Mineral. **60**, 300 (1937).
[15] X. Zhuang, L. Marrucci, and Y. R. Shen, Phys. Rev. Lett. **73**, 1513 (1994).
[16] J. E. Proust, L. Ter-Minassian-Saraga, and E. Guyon, Solid State Commun. **11**, 1227 (1972).
[17] G. Porte, J. Phys. (Paris) **37**, 1245 (1976).
[18] K. Hiltrop and H. Stegemeyer, Ber. Bunsenges. Phys. Chem. **82**, 884 (1978).
[19] K. Hiltrop, J. Hasse, and H. Stegemeyer, Ber. Bunsenges. Phys. Chem. **98**, 209 (1994).
[20] G. P. Crawford, R. J. Ondris-Crawford, J. W. Doane, and S. Zumer, Phys. Rev. E **53**, 3647 (1996).
[21] G. Ryschenkow and M. Kleman, J. Chem. Phys. **64**, 404 (1976).
[22] J. S. Patel and H. Yokoyama, Nature (London) **362**, 525 (1993).
[23] N. A. Clark, Phys. Rev. Lett. **55**, 292 (1985).
[24] G. Friedel, Ann. Phys. (Paris) **18**, 273 (1922).
[25] P. Vetter, Y. Ohmura, and T. Uchida, Jpn. J. Appl. Phys., Part 2 **32**, L1239 (1993).
[26] Y. Ouchi, M. B. Feller, T. Moses, and Y. R. Shen, Phys. Rev. Lett. **68**, 3040 (1992).
[27] J. D. Margerum, A. M. Lackner, E. Ramos, K.-C. Lim, and J. W. H. Smith, Liq. Cryst. **5**, 1477 (1989).
[28] R. Yamaguchi and S. Sato, Jpn. J. Appl. Phys., Part 2 **30**, L616 (1991).
[29] R. Yamaguchi and S. Sato, Jpn. J. Appl. Phys., Part 2 **31**, L254 (1992).
[30] G. Venugopal, S. Krause, and G. E. Wnek, Chem. Mater. **4**, 1334 (1992).
[31] C. G. Garton and Z. Krasucki, Philos. Trans. R. Soc. London, Ser. A **280**, 211 (1964).
[32] P. G. de Gennes and J. Prost, *The Physics of Liquid Crystals* (Oxford, New York, 1993), p. 120.
[33] G. Wulff, Angew. Chem. Int. Ed. Engl. **34**, 1812 (1995), and references therein.